A Study of Stellar Photometric Variability Within the Central 4 pc of the Galactic Center with Infrared Image Subtraction¹

Molly S. Peeples², K. Z. Stanek², and D. L. DePoy²

molly, kstanek, depoy@astronomy.ohio-state.edu

ABSTRACT

We present a catalog of 110 variable stars within $\sim 1'$ of Sgr A* based on image subtraction of near-infrared (H and K) photometry. Our images were obtained over 133 nights from 2000–2002 in H-band and over 134 nights from 2001–2002 in K-band; the typical FWHM is 1.4". We match the catalog to other near-infrared, X-ray, and radio (i.e., maser) data, and we discuss some of the more interesting objects. The catalog includes 14 periodic sources, several known long-period variables and three new LPV candidates. We associate IRS 10* with OH, SiO, and H_2O masers and a bright X-ray point source; this analysis suggests IRS 10* is an AGB star with an accreting companion. Among the \approx 90 newly discovered sources are a probable cataclysmic variable, a potential edge-on contact 84 day period eclipsing binary, and a possible 41 day period pulsating variable.

Subject headings: Galaxy: center — stars: variable

1. Introduction

The Galactic center offers a unique opportunity for studying star formation and stellar populations near a supermassive black hole (SMBH), namely, Sgr A*. Active galactic nuclei and supernovae feedback have been evoked to explain many of the observed inhomogeneities in different galaxies (e.g., Silk 1997; Efstathiou 2000; Scannapieco et al. 2005), but it is only in our own Galaxy that we are able to resolve individual stars within the circumnuclear ring surrounding the central SMBH (Jackson et al. 1993). The cluster of stars at the Galactic center is also unique in that it is comprised of both old and young stars (see e.g., Lacy et al. 1982; Paumard et al. 2006). It is believed that the young stellar population is the result of a burst of star formation at the Galactic center a few megayears ago (Krabbe et al. 1995), and that perhaps Sgr A* was more actively accreting mass then than it is observed to be today. Furthermore, there is evidence that the stellar initial mass function near a SMBH is top heavy (Nayakshin & Sunyaev 2005), implying that the

 $^{^1\}mathrm{Based}$ on observations from the CTIO/Yale 1-m telescope with the ANDICAM imager

²Department of Astronomy, Ohio State University, 140 W. 18th Ave., Columbus, OH 43210

Galactic center is a viable location for finding highly massive stars. Photometric variability is one way of probing the mixed Galactic center stellar population on a large scale, as both evolved low mass (late spectral type) and high mass stars are prone to photometric variations.

There have been several photometric variability studies of the Galactic center. While some of these studies have covered a much longer baseline than ours does (e.g., Ott et al. 1999; Rafelski et al. 2007), with more than 130 epochs in each band, our light curves have a much higher sampling. These data also represent the first major multi-wavelength photometric variability study of the Galactic center since Blum et al. (1996a).

We present here our catalog of 113 variable stars within ~ 2 pc of Sgr A*, including 15 periodic sources. We outline our observations in \S 2. In \S 3 we discuss the reduction of data with image subtraction. We discuss our variable selection in \S 4, and we present the catalog of variables and their light curves along with a discussion of some of the more well-known and interesting objects in \S 5. We adopt a Galactocentric distance of 7.6 kpc (Eisenhauer et al. 2005).

2. Observations

The observations from which IRS 16SW was studied by DePoy et al. (2004) and Peeples et al. (2007) were of a field of view of 112×112 arcseconds (4.12 pc projected) approximately centered on the Galactic center; we describe here the stellar photometric variability in these data. The observations of the Galactic center were made from 2000–2002 at the Cerro-Tololo Inter-American Observatory (CTIO)/Yale 1-m telescope using the facility optical/infrared imager (ANDICAM; see DePoy et al. 2003 for details). ANDICAM has a pixel scale of 0.22'' pix⁻¹ on a 1024×1024 array. Both H- and K-band (centered at 1.6μ m and 2.2μ m respectively) images were taken in the 2001 and 2002 observing seasons; H-band data were also obtained in 2000. The observing campaign consists of every usable night from UTC 2000 August 13 through UTC 2000 October 14, UTC 2001 May 20 through UTC 2001 November 3, and UTC 2002 June 9 through UTC 2002 September 25. Each night, a set of seven slightly offset images were obtained and then combined and trimmed to form a final nightly image. The H-band images consist of 30 s exposures, and it took about four minutes to obtain the group of seven images; the K-band images consist of 10 s exposures and took about two minutes to obtain.

After image quality cuts were made, there are a total of 133 H-band images spanning 774 nights and 134 K-band images spanning 495 nights. The full-width half-maximum (FWHM) ranges from 0″.93 to 1″.93; in general, the H-band images are of somewhat higher quality (typical FWHM \sim 1″.3) than the K-band (with typical FWHM \sim 1″.45). The final H- and K-band images are also offset relative to one another by 8.8″; most of the stars detected in only one of the two bands are due to this offset.

3. Data Analysis

Because the field is crowded, we reduced the data with the ISIS image subtraction package (Alard & Lupton 1998; Alard 2000) following the procedures outlined by Hartman et al. (2004). ISIS measures the change in flux for an object relative to a reference image, after correcting for the relative change in the point spread function (PSF). Our reference images (and thus "fiducial" magnitudes) for both bands are based on images from the 2001 observing season. The reference H-band image is presented in Figure 1.

We identified the stars running DAOPhot/ALLSTAR progam (Stetson 1987, 1992) on the astrometric reference image for each band. The final list consists of 1665 sources in H-band, with $m_H = 9.1$ to 17.0, and 1785 sources in K-band, with $m_K = 7.7$ to 15.1. We based the astrometric and photometric calibration on the 2MASS catalog (Skrutskie et al. 2006). For the astrometry, we obtained an astrometric solution by matching the 2MASS K-band catalog to our K-band data. We similarly solved for the coordinate transformation between the H- and K-band data sets, which enabled us to find the coordinates of sources detected only in H band. The astrometric solution is good to $\pm 0.24''$ in RA and $\pm 0.21''$ in dec (about ± 1 pixel in both coordinates). We calibrated our absolute photometry using this same set of stars matched to the 2MASS catalog; the photometric calibration error is ± 0.03 mag.

We define the limiting magnitude for each band to be where the magnitude distribution peaks, as denoted by the vertical dashed lines in Figure 2; this is approximately the magnitude at which the sky level starts to dominate the signal. The limiting H-band magnitude is 15.1 mag, and the limiting K-band magnitude is 12.6 mag; because these magnitude determinations are based on composite images (as opposed to individual images), the actual limiting magnitudes for individual observations of variable sources are significantly lower. The color-magnitude diagram is presented in Figure 3.

4. Variable Selection

The easiest to identify variable stars are those which vary about a mean magnitude more than typical stars of the same average mangitude. We therefore flagged potential variables independently in both H- and K-bands according to an root-mean-squared (rms) cut, as shown in Figure 4. The cutoffs are given by

$$\log(\text{rms, H}) \ge 0.377 \, m_H - 6.044 \quad \text{and}$$
 (1)

$$\log(\text{rms, K}) \ge 0.370 \, m_K - 5.192.$$
 (2)

This led to 238/1665 = 14.3% of H-band sources and 223/1785 = 12.5% of K-band sources being flagged as potential variables. Each potential variable was visually inspected by two of us (M.S.P. and K.Z.S.), and flagged as "periodic" (if an AoV test yielded a believable period), "long term," "suspected," or not variable. We also performed two period searches (AoV and LS;

Schwarzenberg-Czerny 1996; Scargle 1982) of all of the sources. These searches revealed only two periodic sources not already flagged by the rms cut as well as three other clearly variable, low-amplitude non-periodic sources. The final sample includes 93 sources with both H- and K-band light curves, 14 of which are periodic, as well as 10 stars identified only in H-band and 7 stars identified only in K. The distribution of magnitudes for all of the variable sources are shown as the shaded regions of the histograms in Figure 2.

Several of the sources flagged as variables were clearly blended, i.e., nearby stars show similar light-curve shapes. As described in § 4.6 of Hartman et al. (2004), the true variable is the one which displays the greatest amplitude of variability in flux. Thus, while in most cases we have not attempted to correct for blending, we are able to identify which sources are the true variables.

5. Catalog of Variables

The positions and magnitudes of our non-perioidic variable sources are given in Table 1, and the light curves¹ are shown in Figure 5, 6, and 7. The periodic sources are summarized in Table 2 and Figure 8.

In this section, we discuss indvidual interesting variable sources. For previously identified sources, we compare our data to other studies. Table 3 summarizes some of the main near-infrared variability surveys of the Galactic center to date. At higher energies, Muno et al. (2004) used the Chandra X-Ray Observatory to study X-ray sources in the 0.5–8.0 keV band in the central 9' of the Galaxy from September 1999 to June 2002. Of the more than 2000 point sources studied, 77 sources at the Galactic center displayed long-term variability. On the other end of the spectrum, several masers have been identified at the Galactic center. Specifically, Sjouwerman et al. (2002) studied 25 22 GHz H₂O masers within 2° and 18 43 GHz SiO masers within 15' of Sgr A*; these masers are associated with OH stellar masers found by Lindqvist et al. (1992).

A summary of the sources discussed in this section is presented in Table 4; we first discuss previously identified sources, starting with the IRS sources (sorted numerically), followed by several sources also found by Glass et al. (sorted by their Samus & Durlevich 2004 variable catalog name). Finally, we discuss some of the more interesting new variables in our catalog; these subsections are sorted by RA, as in Tables 1 & 2.

5.1. IRS 1NE

IRS 1NE (PSD J174540.58-290026.7) passes the rms cut described in § 4, but visually does not appear to vary over the timescales to which we are sensitive in this study. Ott et al. (1999)

 $^{^1}$ Full light curves are available upon request from M. Peeples at molly@astronomy.ohio-state.edu.

similarly found IRS 1NE to pass their χ^2 variability cut, but this source did not pass their visual inspection test either. It is possible that IRS 1NE is in fact variable, but over shorter timescales to which either Ott et al.'s or our survey was sensitive, i.e., $\lesssim 1$ day.

5.2. IRS 7

IRS 7 (PSD J174540.04-290022.7) is the brightest source in the field, and the only one to saturate in our K-band images. Ott et al. (1999) find this M2 supergiant long-period variable (LPV) to have a $\Delta m_K = 0.26$. We find a $\Delta m_H = 0.33$ (from $m_H = 9.0$ to 9.33).

5.3. IRS 9

IRS 9 (PSD J174540.47-290034.6) is a large-amplitude variable, with $\Delta m_H = 0.92$ mag and $\Delta m_K = 0.22$ mag (though most of the H-band large amplitude variability is seen in the year 2000, when no K-band data were taken). In our data, IRS 9 is blended with two stars detected in only H-band. Blum et al. (1996a) found the H-K color of this M7 LPV to change by ~ 0.2 mag from September 1989 to July 1993. Tamura et al. (1996) find IRS 9 to have brightened by ≈ 0.37 mag in K-band over about two years (from 1991 to 1993). Glass et al. (2001) find IRS 9 (their 3-2753, also known as V4920 Sgr) to have $\Delta m_K = 0.55$ mag over a period of 463 days; while our data do not rule out such a period, the light curve appears more consistent with that of a large-amplitude irregular variable.

5.4. IRS 10*

Tamura et al. (1996) found a variable source between IRS 10E and IRS 10W. Dubbed² IRS 10*, its brightness increased by at least one magnitude between 1991 and 1992. Ott et al. (1999) found similar long-period brightness variations on the order of 1.4 mag. Like Tamura et al., we do not separately resolve IRS 10E, 10W, and 10*. In the subtracted images from ISIS, there appears to be only one point-source of variability in the IRS 10 region (i.e., IRS 10E and 10W are presumably non-varying). We associate this variability seen in the IRS 10 complex with IRS 10*, even though DAOPhot detects two sources in H-band (apparently the brighter nearby IRS 10E and 10W) and only one source in K-band. Because of this, the position we state for IRS 10* (PSD J174540.64-290023.6) in Table 1 is from Ott et al. (1999); the stated K-magnitude (10.2) is probably largely due to IRS 10E. We find the K-magnitude of IRS 10* to be relatively constant in both the 2001

 $^{^{2}}$ This source is referred to in the literature as IRS 10E*, IRS 10EL, and IRS 10EE; we will use here the original name IRS 10*.

and 2002 observing seasons, with the 2002 value being ~ 0.8 mag brighter. Furthermore, IRS 10* was much redder in 2002 than it was in 2001.

Both Tamura et al. and Ott et al. associated IRS 10* with the OH maser OH 359.939-0.052 (Lindqvist et al. 1992), but Blum et al. (1996a,b) associated it with the Lindqvist et al. (1992) maser OH 359.946-0.047³. Menten et al. (1997) found an SiO maser and Lindqvist et al. (1990) found a H₂O maser coincident with OH 359.946-0.047; Deguchi et al. (2002) and Sjouwerman et al. (2002) further found the SiO maser and the H₂O maser to be variable, respectively. Muno et al. (2004) additionally identify an X-ray source, CXOGC J174540.7-290024, within 0.8" of IRS 10* with an (unobscured) X-ray luminosity $L_X \approx 1.1 \times 10^{32} {\rm erg~s^{-1}}$. Typically OH/IR stars are asymptotic giant branch (AGB) stars; these pulsating stars are experiencing mass loss, which accounts for both the NIR variability and the presence of masers. Genzel et al. (1996) spectroscopically confirm that IRS 10* (their IRS 10EE) is a late-type (i.e., consistent with being an AGB) star.

While it is possible that the X-ray flux is due to some other nearby source (or collection of sources), under the assumption that all three masers and the X-ray source are associated with IRS 10* (and not IRS 10E or 10W), this might be the largest X-ray luminosity associated with an AGB star to date (Karovska et al. 2005). It has been proposed that AGB stars should be bright Xray sources $(L_X \sim 10^{31} - 10^{35} \text{ erg s}^{-1})$ due to strong magnetic fields, but various X-ray studies have not confirmed this prediction (e.g., Soker & Zoabi 2002; Kastner & Soker 2004a,b); typical X-ray luminosities for, e.g., Mira, are $\sim 10^{29} \text{ erg s}^{-1}$ (Kastner & Soker 2004b). Soker & Zoabi suggest that AGB stars are radiating in the X-ray as proposed, but this radiation is not observed due to the high column density of the ejected material surrounding the star (see also Blackman et al. 2001). Furthermore, all AGB stars with detected X-ray radiation are in binary systems (e.g., Mira A & B, Karovska et al. 2005); if this trend is in fact a prerequisite for a high X-ray luminosity, then IRS 10* should have a companion. Because SiO, H₂O, and OH masers are believed to be due to different regions of the circumstellar envelope (SiO masers are relatively close to the star, H₂O masers are further out, and OH masers are even further away from the star Reid & Moran 1981), the presence of all three masers implies that IRS 10* is enshrouded by a substantial circumstellar envelope; yet as this material does not absorb the X-ray radiaion, the X-ray flux is more likely to be due to accretion onto a companion star than the AGB itself.

5.5. IRS 12N

Tamura et al. (1996), Blum et al. (1996a), Ott et al. (1999), and Glass et al. (2001) found IRS 12N (PSD J174539.79-290035.2, spectral type M7III) to be variable. Tamura et al. (1996) observed an increase of $\Delta m_K \sim 0.47$ mag over 2 years, and Ott et al. (1999) found similar variations.

³Though they are only two lines apart in Lindqvist et al.'s Table 2, OH 359.939-0.052 is roughly 35" further from the IRS 10 complex than OH 359.946-0.047.

Glass et al. (2001) found IRS 12N (their 3-2753) to be a periodic variable of similar magnitude ($m_K = 8.74$) and amplitude ($\Delta m_K = 0.55$ mag) with a period P = 463 days. We cannot deblend IRS 12N and IRS 12C; five variable sources are detected within $\sim 1.5''$ of IRS 12N with similar features to one another. We find this source to potentially be periodic, with P = 215 or 429 days and a $\Delta m_K \gtrsim 0.4$ mag and a $\Delta m_H \gtrsim 0.65$; no variations are observed on shorter timescales. These data are in agreement with the classification of IRS 12N as an LPV (Blum et al. 1996b).

5.6. IRS 14SW

IRS 14SW (PSD J174540.02-290037.2) is seen to have variability with amplitude ~ 0.1 mag in both H- and K-bands in the 2001 and 2002 observing seasons. Additionally, the H-band lightcurve is ~ 0.1 mag lower in the 2000 observing season than in 2001–2002. Tamura et al. (1996) state that IRS 14SW is a "probable" variable; Ott et al. (1999) find that IRS 14SW passes their χ^2 cut, but they do not comment on its variability. It is clear from our data that IRS 14SW is, in fact, a variable source.

5.7. IRS 14NE

IRS 14NE (PSD J174540.11-290036.4) is a known AGB star (spectral type M7III; Blum et al. 1996b). Ott et al. (1999) find IRS 14NE to have $m_K = 9.45$ mag and amplitude $\Delta m_k = 0.15$, though they do not flag it as a potential variable. This is consistent with our findings of $\Delta m_k \approx 0.14$ and $\Delta m_H \approx 0.16$; we find its variability to have clear structure.

5.8. IRS 15SW

IRS 15SW (PSD J174539.99-290016.5) is a known Wolf-Rayet (WR) star (also known as WR 101i; van der Hucht 2001) with spectral type WN8/WC9 (Najarro et al. 1997; Paumard et al. 2006). We detect small-amplitude variations in IRS 15SW, with $\Delta m \sim 0.15$ mag.

5.9. IRS 16NE

Like many of the stars in the IRS 16 cluster, IRS 16NE (PSD J174540.25-290027.2) is a potential luminous blue variable (LBV) star (Clark et al. 2005) with spectral type Ofpe/WN9 (Paumard et al. 2006). We observe IRS 16NE to have an amplitude of only ~ 0.11 mag in both H and K; furthermore, we do not observe the H-K color to change substantially or systematically. On the other hand, the light curve is potentially consistent with a period of 205 days.

5.10. IRS 16SW

IRS 16SW (PSD J174540.12-290029.6) was originally proposed to be a massive eclipsing binary by Ott et al. (1999). Using the same data presented here, DePoy et al. (2004) proposed that IRS 16SW is instead a new kind of massive pulsating star, but a recent re-reduction of the data by Peeples et al. (2007) revealed a sign error in the DePoy et al. analysis. Martins et al. (2006) presented a radial velocity curve of IRS 16SW; while it appears to be a single-line binary, both their analysis and that of Peeples et al. found the data to be consistent with a contact binary of twin $50M_{\odot}$ stars. While Rafelski et al. (2007) also support the idea that IRS 16SW is an eclipsing binary, their light curve shows an asymmetry in the rise- and fall-times—the rise-time appears to be ~ 1.6 times that of the fall-time—which they propose is due to tidal deformations causing asynchronous rotational and orbital periods of the two stars. As discussed by Peeples et al., our data do not show such a strong asymmetry; such an asymmetry is not seen by Martins et al. either.

5.11. IRS 28

IRS 28 (PSD J174540.83-290034.0) is another source described as a "probable" variable by Tamura et al. (1996). Blum et al. (1996b) classify IRS 28 as an LPV, and Glass et al. (2001) find IRS 28 (their 3-72, also known as V4923 Sgr) to be a periodic source with an amplitude of $\Delta m_K = 0.4$ mag and a period of P = 195 days. We find this source to *not* be clearly periodic (and a period of ~200 days is ruled out). We find $\Delta m_K \sim 0.2$ mag and $\Delta m_H \approx 0.32$ mag; in the two observing seasons with both H- and K-band data, the two lightcurves have similar structures, but the H-band lightcurve clearly has a larger amplitude.

5.12. IRS 34W

Trippe et al. (2006) find IRS 34W (PSD J174539.76-290026.4) to be an irregular variable Ofpe/WN9 star, suggesting that it is a transitional object between the O supergiant and LBV phases of its evolution. We find an H - K color of 3.5 mag, which is consistent with what Trippe et al. found for a similar epoch.

5.13. V4910 Sgr and V4911 Sgr

Glass et al. (2001) found V4910 Sgr (their 3-270, our PSD J174537.24-290045.7) to have a $m_K = 10.27$ and vary with amplitude 0.8 mag over a period of 601 days. We find V4910 Sgr to have $m_H = 12.6$ and $m_K = 9.9$, with amplitudes $\Delta m_H = 0.73$ mag and $\Delta m_K = 0.56$ mag. While a period of ~ 600 days is not ruled our by our data, this source appears to be an irregular large-amplitude variable with no convincing signs of periodicity.

Similarly, Glass et al. found V4911 Sgr (their 3-88, our PSD J174538.02-2901002.6) to have a $m_K = 9.58$ with amplitude 0.5 mag over a period of 528 days. We find V4911 Sgr to have $m_H = 12.5$ and $m_K = 9.3$, with amplitudes $\Delta m_H \approx 1.15$ mag and $\Delta m_K = 0.58$ mag (much of the variation seen in H-band is from the 2000 observing season, when no K-band data were taken). While a period of ~ 528 days is not ruled out by our data, this source appears to be an irregular large-amplitude variable with no convincing signs of periodicity. Deguchi et al. (2002) associate V4911 Sgr with the SiO maser SiO 359.930-0.045, though the projected separation is $\sim 7''$.

5.14. V4928 Sgr

PSD J174542.72-285957.4 is one of the brightest stars in our sample. Also known as V4928 Sgr, this source is associated with OH, SiO, and H₂O masers, OH 359.956-0.050⁴ at $\alpha = 17^{\rm h}45^{\rm m}42.763^{\rm s}$, $\delta = -28^{\circ}59'57.20''$ (Deguchi et al. 2002; Sjouwerman et al. 2002). Glass et al. (2001) find V4928 Sgr (their 3-5) to have an m_K of 7.89 mag, with amplitude $\Delta m_K = 0.65$ mag and period P = 607 days. We find amplitudes of $\Delta m_H \approx 0.4$ mag and $\Delta m_K \approx 0.25$ mag, but it is clear that the "true" amplitude is greater than this, as at the end of the 2001 observing season the light curve shows no signs of flattening. Though a period of ~ 600 days does not appear consistent with our data, we cannot rule out that V4928 Sgr is indeed periodic. The observed large-amplitude variability in the presence of masers flags this source as an LPV candidate.

It is possible that V4928 Sgr is, in fact, the LPV IRS 24 (Blum et al. 1996a,b). The projected distance between IRS 24 (at $\alpha=17^{\rm h}45^{\rm m}41.8^{\rm s}$, $\delta=-28^{\circ}59'59.51''$ J2000.0) and V4928 Sgr is 13.6"; however, when Levine et al. (1995) first discovered an H₂O maser at $\alpha=17^{\rm h}45^{\rm m}42.7^{\rm s}$, $\delta=-28^{\circ}59'57.2''$ J2000.0, they associated it with the bright near-infrared IRS 24.

5.15. V4930 Sgr

V4930 Sgr (PSD J174543.19-290013.0) is a known Mira (LPV) variable (Samus & Durlevich 2004). We observe V4930 Sgr, which is one of the brighest variable stars in our sample, to smoothly vary with an amplitude of ~ 1 mag in H and ~ 0.7 mag in K. Glass et al. (2001) likewise find V4930 Sgr (their 3-16) to have an amplitude of $\Delta m_K = 1.0$ mag over a period of 554 days. While our H-band data do not rule out a period of ~ 550 days, the light curve does not appear to be clearly periodic.

⁴Ott et al. (1999) associate this maser with IRS 10*, but they are separated by $\approx 35''$.

5.16. PSD J174535.60-290035.4 and PSD J174538.34-290036.7

PSD J174535.60-290035.4 and PSD J174538.34-290036.7 are two of the most enigmatic variables in our sample. For simplicity, in this section alone, we will refer to PSD J174535.60-290035.4 as PSD 35.6-35.4 and PSD J174538.34-290036.7 as PSD 38.3-36.7. Both of these variables are clearly periodic. PSD 35.6-35.4 has a period $P = 41.3 \pm 0.5$ days with amplitude $\Delta m_K \approx 0.77$ and $\Delta m_H \approx 0.63$; PSD 38.3-36.7 has a period $P = 42.4 \pm 0.8$ days with amplitudes $\Delta m_K \approx 0.66$ and $\Delta m_H > 0.57$ mag (PSD 38.3-36.7 is quite faint in H-band). Because these periods, magnitudes, and variability amplitudes are so similar, we will discuss these two sources together.

One obvious intriguing possibility is that these stars are Cepheids. Both of these sources have $\langle m_K \rangle \approx 12.3$ mag; assuming these are Cepheids and taking P=42 days, we can calculate the absolute K-band magnitude using the Cepheid period-luminosity relation from Hindsley & Bell (1990):

$$\langle M_K \rangle = -3.80[\log(P) - 0.8] - 5.46 = -8.59.$$
 (3)

If we now assume that these stars are at the Galactic center, with $d_{GC} = 7600$ pc, we can take this absolute magnitude and calculate the K-band extinction,

$$A_K = \langle m_K \rangle - \langle M_K \rangle - 5 \log d_{GC,pc} + 5 = 6.46. \tag{4}$$

This A_K , which corresponds to an $A_V = A_K/0.112 = 57.7$ (Schlegel et al. 1998), is rather large, even for the Galactic center. Scoville et al. (2003) give A_V near PSD 38.3-36.7 to be ~ 25 (derived from Pa α to H92 α radio recombination line-emission ratios) to ~ 34 (derived from Pa α to 6 cm radio continuum emission ratios); A_V is unmeasured near PSD 35.6-35.4. Another way of expressing this discrepancy is to say that if we use the Scoville et al.'s average A_K for the field, $A_K = 3.48$, then equation (4) yields an $\langle M_K \rangle$ that is ≈ 3 mag fainter than is predicted by equation (3).

It is possible, of course, that the intervening dust is patchy on scales smaller than Scoville et al. (2003) could resolve, and that one or both of these stars happens to be behind a dense clump of obscuring material. Under the assumption that these stars are Cepheids, we can constrain the actual A_K for each source from the observed H-K colors; Cepheids have an unreddened $\langle M_H-M_K\rangle\approx 0.0$ (Laney & Stobie 1994). Taking $A_H/A_V=0.176$ and $A_K/A_V=0.112$ from Schlegel et al. (1998), we find

$$A_K = \frac{E(H - K)}{0.176 - 0.122} \times 0.112 = 1.75E(H - K). \tag{5}$$

For $M_H - M_K = 0.0$, the observed H - K color of 2.2 for PSD 35.6-35.4 yields $A_K = 3.85$ and the observed H - K color of 2.6 for PSD 38.3-36.7 yields $A_K = 4.55$. These extinction values are substantially less than the $A_K = 6.46$ calculated above; if either of these stars is in fact a Cepheid, some combination of a different reddening law or a different period-luminosity relation than used here would have to come into play.

If neither PSD 35.6-35.4 nor PSD 38.3-36.7 is a Cepheid, then the possible nature of the variability seen in these stars is unclear. The shape of the light curve of PSD 35.6-35.4 remains

reminiscent of a pulsating variable; a steep brigtening is followed by a longer fall-time. The light curve of PSD 38.3-36.7, however, is much more symmetric; it is possible that it is an eclipsing binary. If this is the case, then like IRS 16SW (see §§ 5.10) it is both close to in contact (because the light curve does not flatten out of eclipse), composed of equal surface brightness stars (because the depths of the eclipses are the same), and we are viewing it almost edge-on (because the depths of the eclipses are close to 0.75 mag). These conditions are suspicious given that, if PSD 38.3-36.7 is a binary, then its period is 84.8 days. For comparison, IRS 16SW has a period of 19.45 days and is comprised of two $50M_{\odot}$ stars with a separation of $\sim 150R_{\odot} \approx 0.7$ AU (Martins et al. 2006; Peeples et al. 2007). Spectroscopic monitoring is the only way to determine the nature of the variability of PSD 35.6-35.4 and to break the mass-radius degeneracy if PSD 38.3-36.7 is an eclipsing binary.

5.17. PSD J174538.98-290007.7

We observe PSD J174538.98-290007.7 to have a period of ≈ 325 days with an amplitude of 0.75 mag in H-band and 0.52 mag in K-band. Based on this large period and these large amplitudes of variation, we propose that PSD J174538.98-290007.7 is an LPV.

5.18. PSD J174537.98-290134.4 and PSD J174539.31-290016.3

We associate PSD J174537.98-290134.4 and PSD J174539.31-290016.3 with CXOGC J174537.9-290134 and CXOGC J174539.3-290016 respectively (Muno et al. 2004). PSD J174537.98-290134.4 has marginal variability, but it is a bright source ($m_H = 9.5$ and $m_K = 8.6$). Muno et al. detected neither short-term nor long-term variability for either X-ray source.

5.19. PSD J174540.16-290055.7

PSD J174540.16-290055.7 is, within uncertainties, coincident with the long-term X-ray variable CXOGC J174540.1-290055 ($L_X \sim 10^{35} {\rm erg \ s^{-1}}$, Muno et al. 2004). We find this source to potentially be periodic, with a period of ≈ 215 days and an amplitude of $\Delta m_H = 0.2$ mag and $\Delta m_K = 0.15$ mag. Muno et al. observed the X-ray flux, on the other hand, to vary by a factor of five over the course of 17 days. These data are consistent with PSD J174540.16-290055.7 being a bright cataclysmic variable; the observed period of ≈ 215 days is potentially the orbital period of the evolved star around an accreting white dwarf.

5.20. PSD J174541.39-290126.6

PSD J174541.39-290126.6 is one of the reddest stars in our sample, with an observed H - K = 4.3 mag. In H-band we observe an amplitude of ~ 1 mag, though the more coherent K-band light curve only shows variations of $\Delta m_K \approx 0.6$ mag. Both Wood et al. (1998) and Glass et al. (2001) find this object (their 61-7 and 3-205 respectively) to have an amplitude of ~ 0.8 –0.9 mag and a period of ≈ 515 days, both of which are consistent with our data. Furthermore, Wood et al. associate this large-amplitude variable with the OH/IR star OH 359.932-0.059 (Sjouwerman 1997).

5.21. PSD J174542.36-290011.2

PSD J174542.36-290011.2 is a periodic source with $P \sim 220$ days and amplitudes $\Delta m_H = 0.61$ mag and $\Delta m_K = 0.45$ mag. PSD J174542.36-290011.2 shows regular brightness variations over a period of 110.8 days, but when phased at a period of 221.6 days, both the maxima and the minima are less extreme in the first half of the oscillation than in the second. While minima alternating between shallow and deep is characteristic of an RV Tauri type star, a period of ~ 220 days is too long for PSD J174542.36-290011.2 to be an RV Tauri type star (Sterken & Jaschek 1996).

5.22. PSD J174543.14-290050.2

We observe PSD J174543.14-290050.2 to have amplitudes of $\Delta m_H \sim 0.9$ and $\Delta m_K \sim 0.6$ mag. While it does appear to be periodic, the actual period is not clear; it is possible that the period varies from cycle to cycle. Based on these observations, we propose that PSD J174543.14-290050.2 is an LPV.

6. Summary

We present a catalog of variable stars within ~ 2 pc of Sgr A* in the near-infrared H and K bands over a three-year baseline; $\approx 80\%$ of these variables are previously unidentified. This is the first photometric variability study of the Galactic center to use the technique of image subtraction.

We find several new periodic sources. Of these, PSD J174535.60-290035.4 and PSD J174538.34-290036.7 have the shortest periods, with $P \sim 42$ days. We believe PSD J174535.60-290035.4 is a pulsating variable, though it is unlikely to be a Cepheid. PSD J174538.34-290036.7 appears to be a nearly edge-on contact eclipsing binary system, in which case the period is actually 84.8 \pm 1.6 days and the individual components are likely to be quite large. Another periodic source, PSD J174540.16-290055.7 ($P \approx 215$ days), is coincident with the X-ray variable CXOGC J174540.1-290055; we suspect that this source is a cataclysmic variable. Among the previously identified sources in the catalog, we associate IRS 10* with a bright X-ray point source and OH, H₂O, and

SiO masers, suggesting that it is an AGB star with an accreting companion.

David Gonzalez and Juan Espinoza collected all the imaging data used in this paper, and we are grateful for their dedication and competence. The CTIO/Yale 1.0m telescope and ANDICAM are operated by the SMARTS consortium. We would like to thank Vincent Fish for explaining masers and Marc Pinsonneault for explaining stars to us. We also thank Joel Hartman for his useful flux2mag and vartools programs, Grzegorz Pojmanski for his excellent lc program, and Andy Gould and Rick Pogge for helpful discussions.

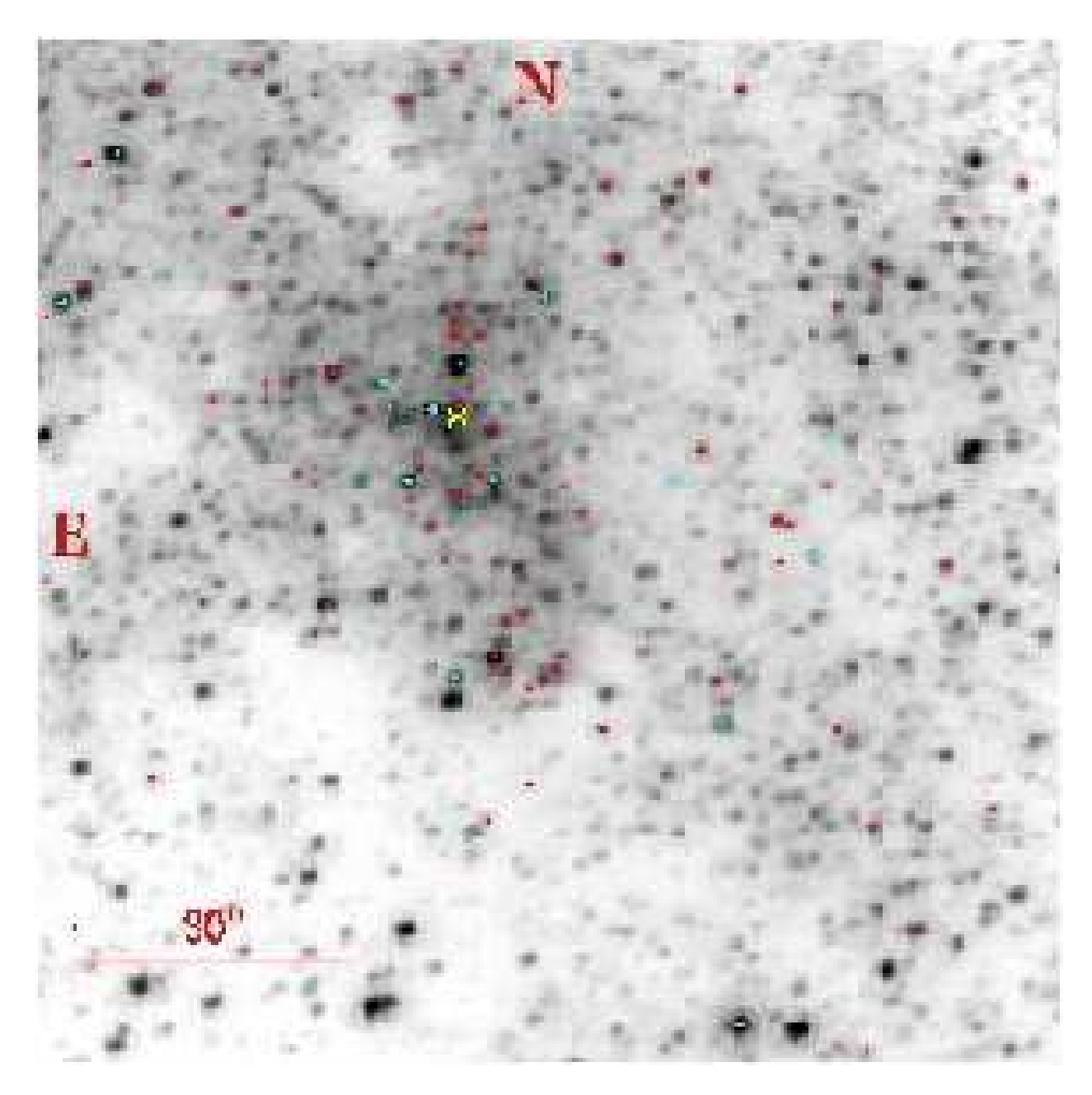


Fig. 1.— The reference H-band image. The red and cyan points mark variable sources listed in Tables 1 & 2; the cyan points mark stars discussed in \S 5. The yellow X marks the location of Sgr A*. North is up and East is to the left.

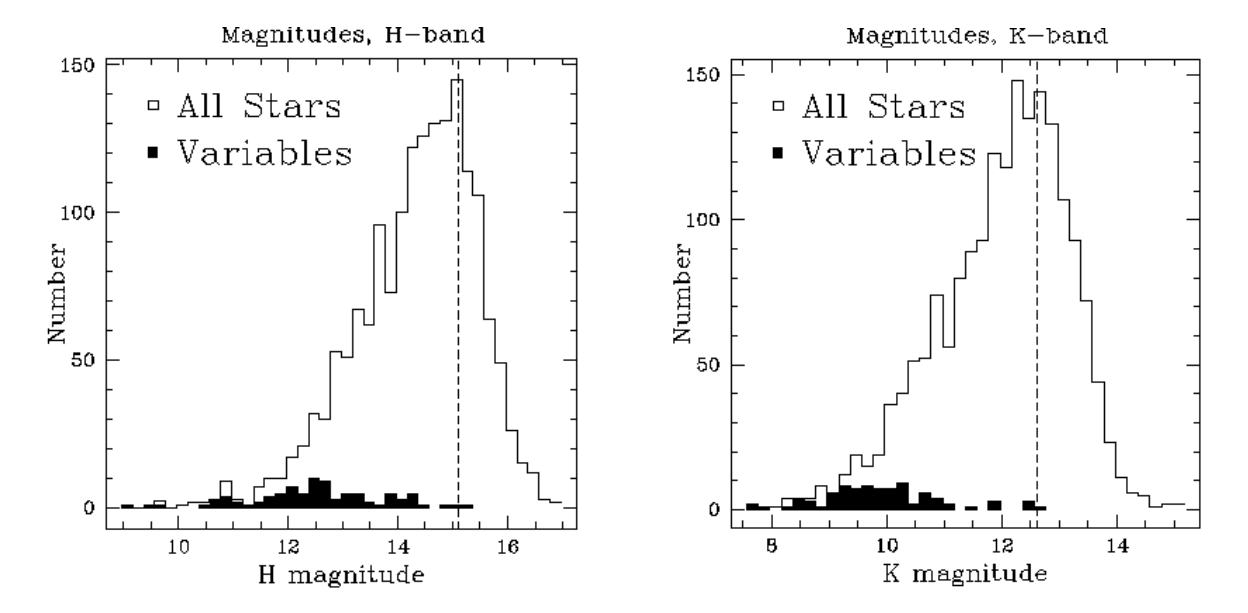


Fig. 2.— Distribution of magnitudes in H band (left) and K band (right) for all detected sources. The vertical dashed lines are at the limiting magnitude for each band (see \S 3). The shaded histograms are the distribution of all variable sources; the variable sources fainter than the limiting magnitude are those sources which, while detected in both bands, are brighter than the limiting magnitude in one band, but below the limiting magnitude in the other band.

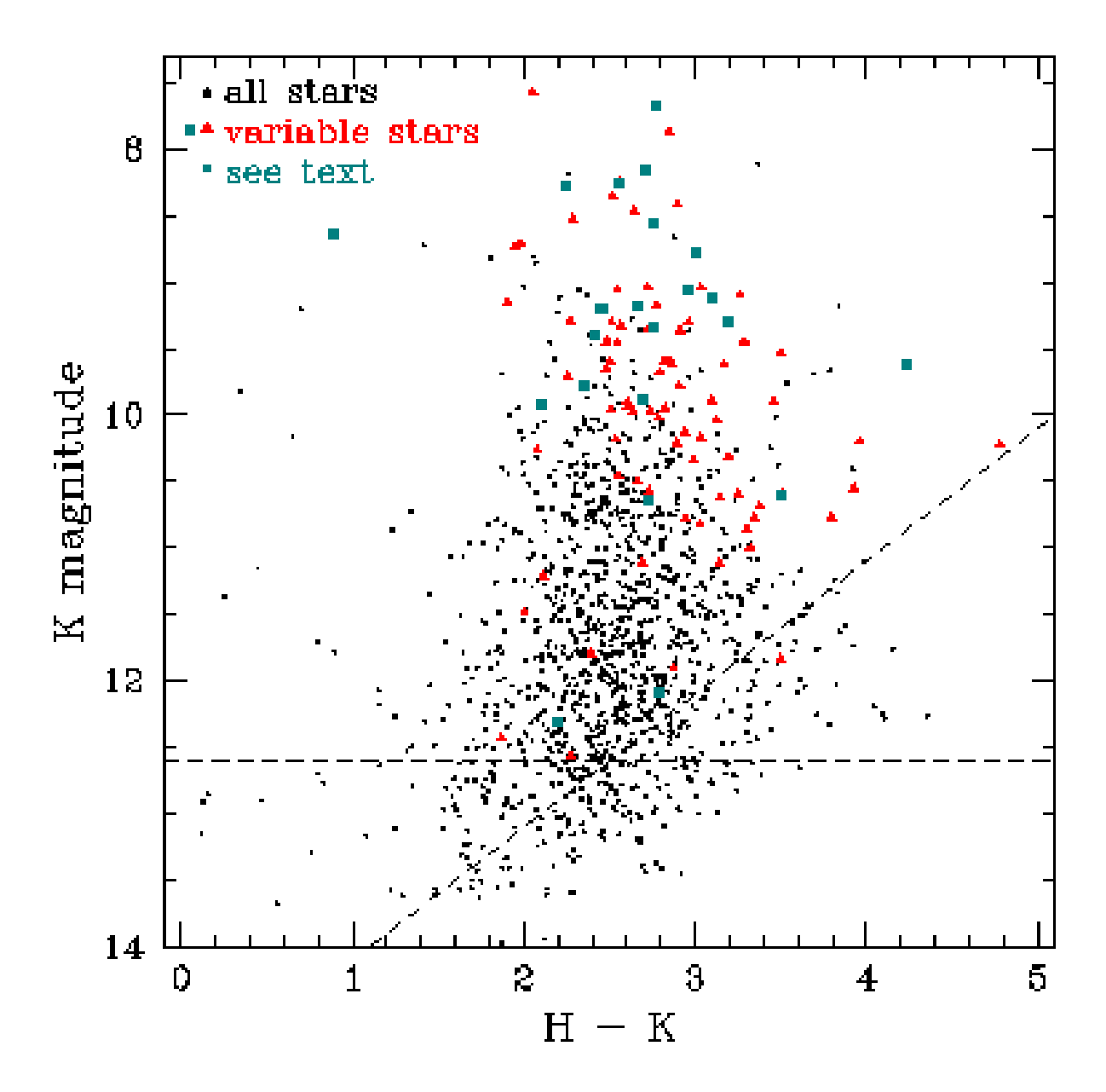


Fig. 3.— Color-magnitude diagram. The red triangles and the cyan squares are variable sources; the cyan squares are the variable sources discussed in \S 5. Most of the spread in H-K is due to differential reddening; the dashed lines correspond to the magnitude limits discussed in \S 3.

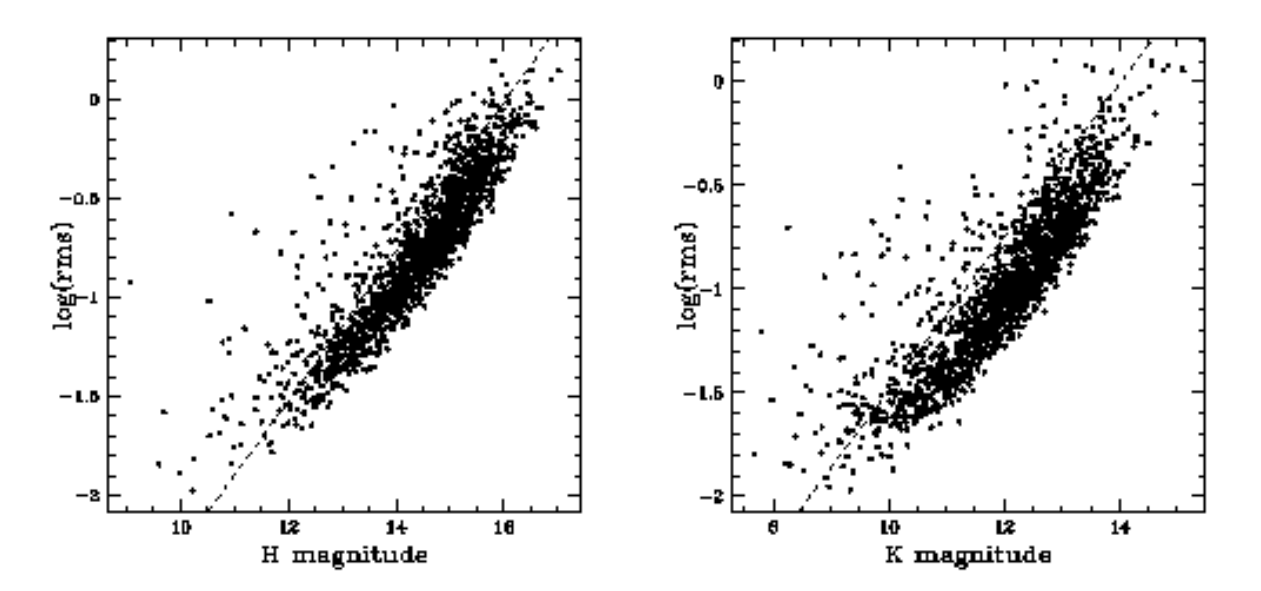


Fig. 4.— Plots of log rms v. magnitude for H (left) and K (right). Stars lying above the line were flagged as "potential variables."

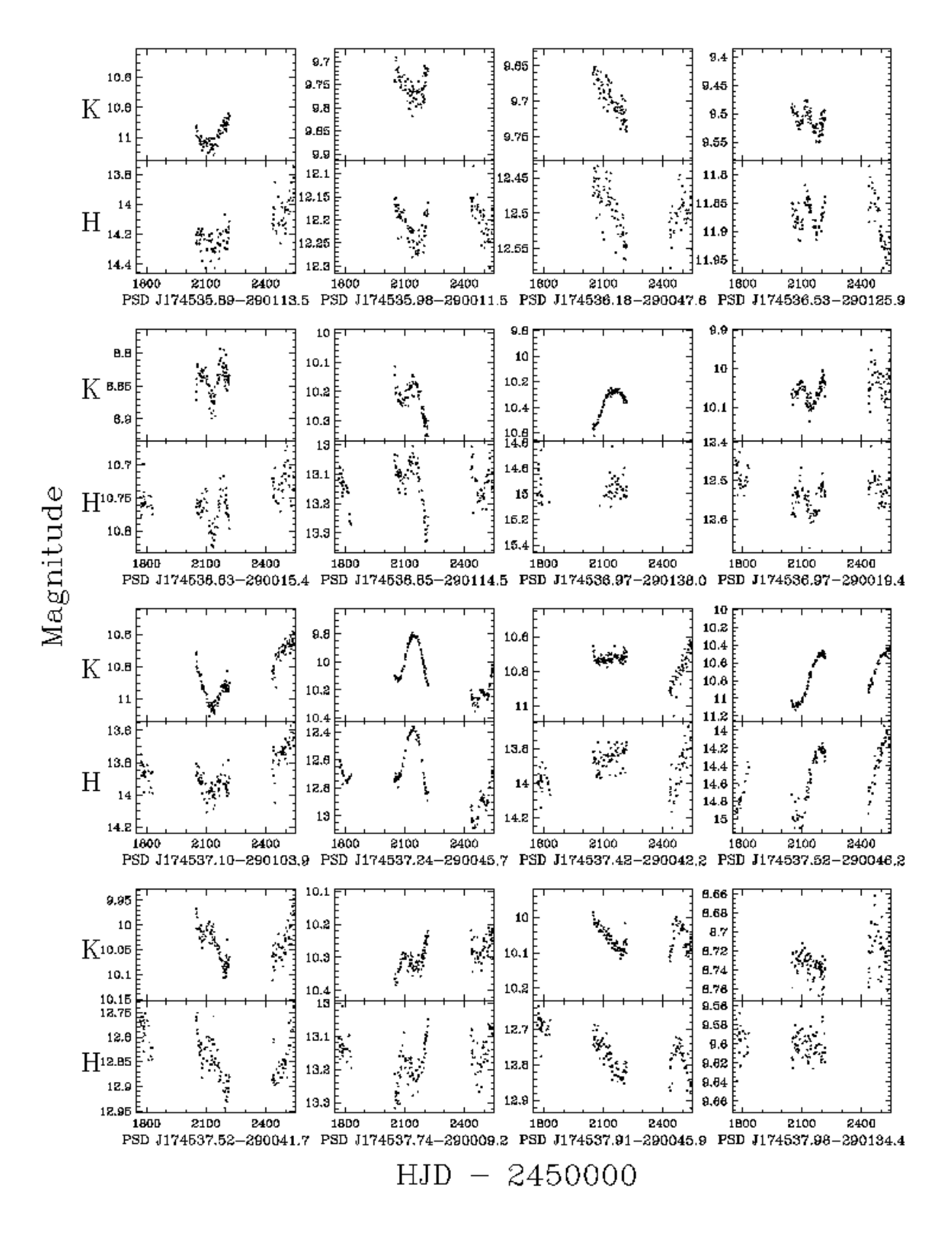


Fig. 5.— (a)—Light curves of non-periodic sources detected in both H and K, sorted by RA as in Table 1. For each source, the extent of the H- and K-band ranges plotted is the same. Points lying below the magnitude limit (see \S 3) are not included.

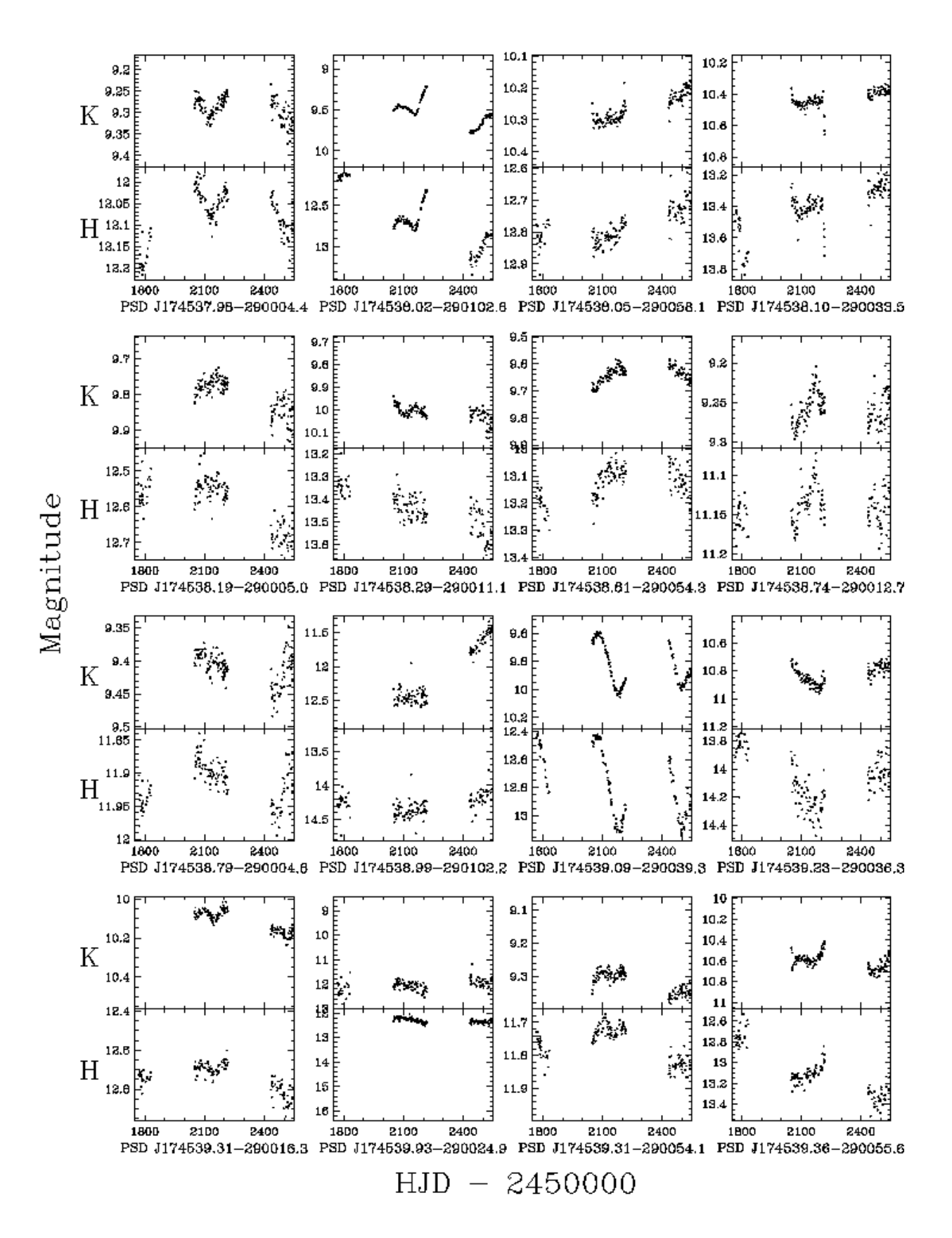


Fig. 5.— (b)

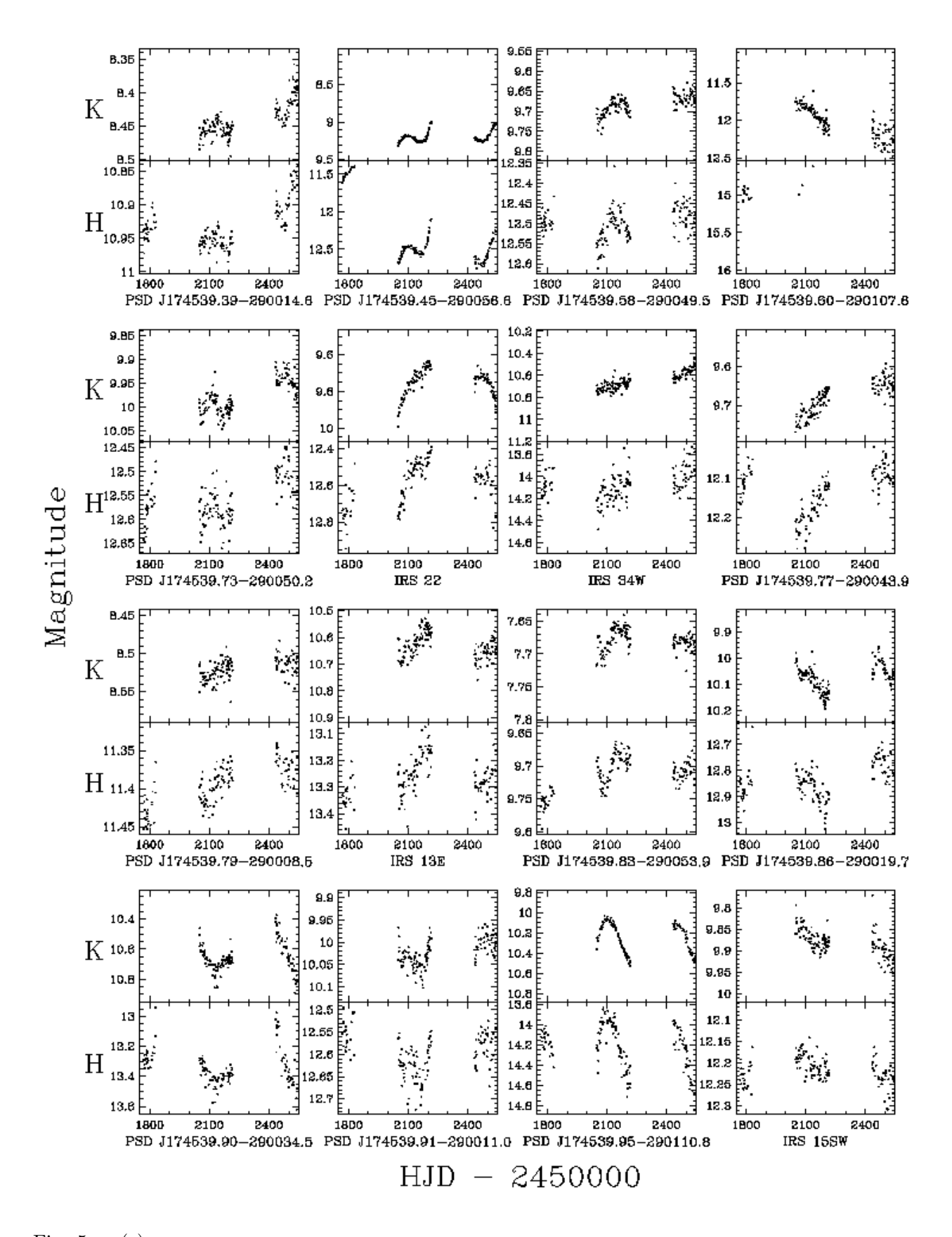


Fig. 5.— (c)

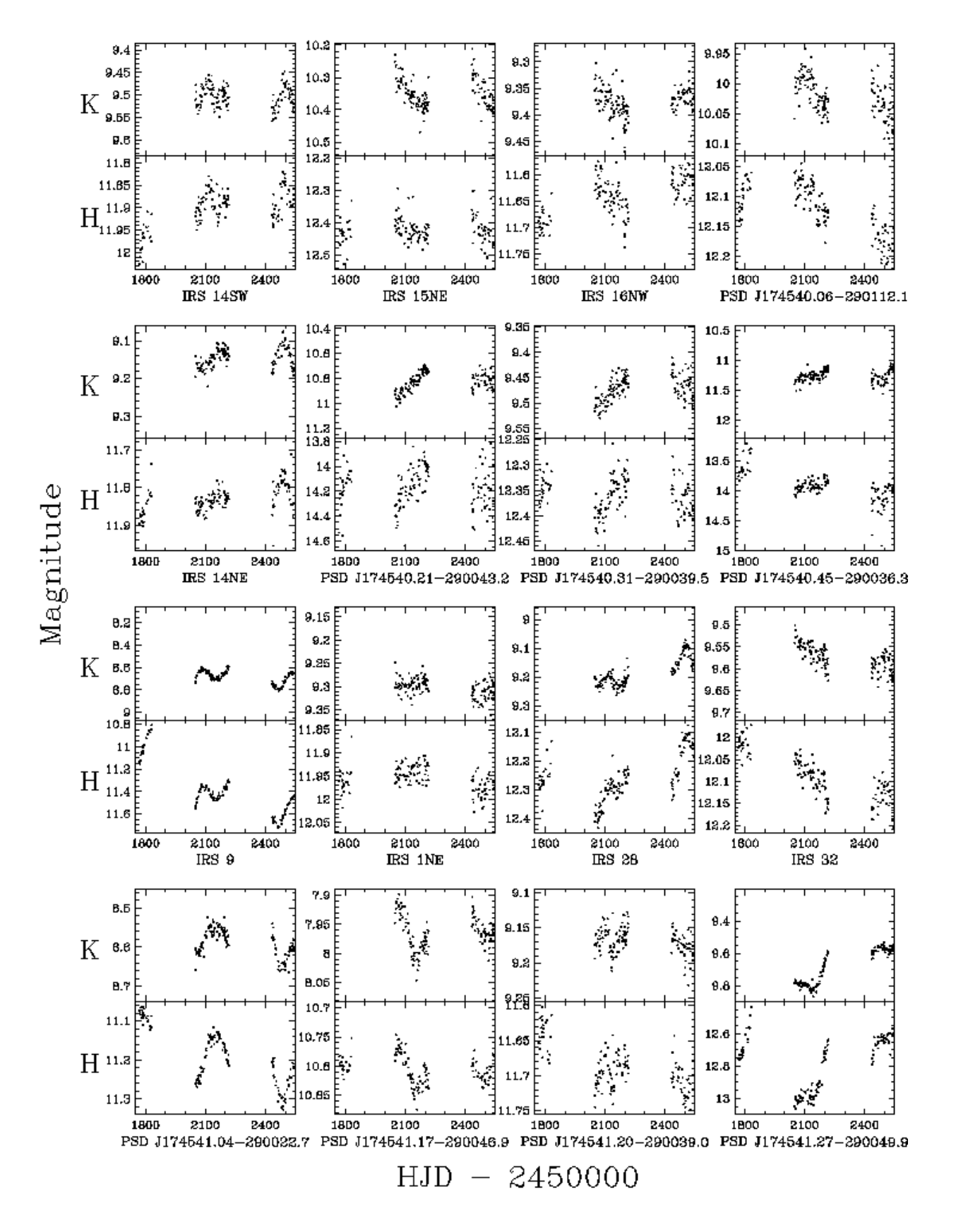


Fig. 5.— (d)

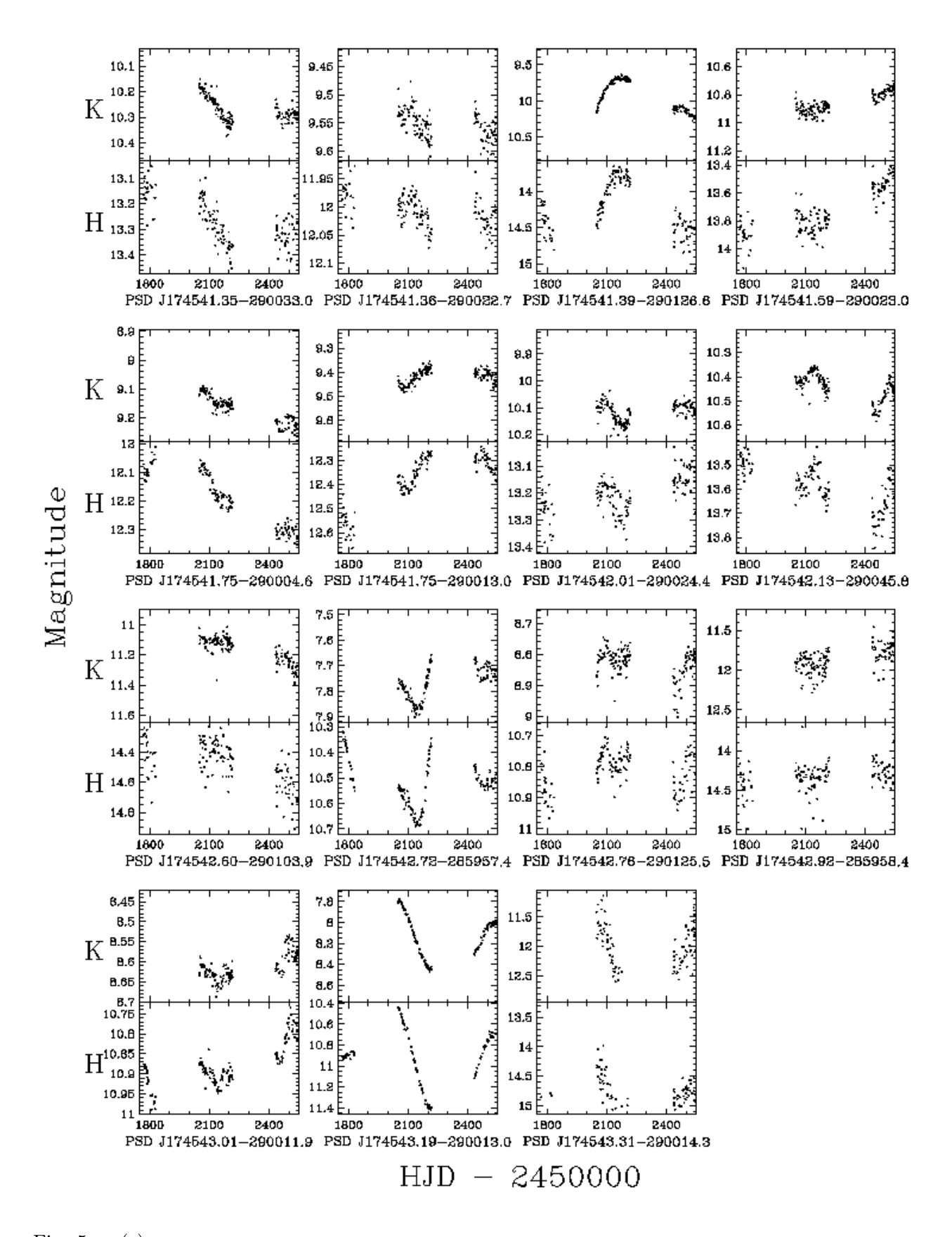


Fig. 5.— (e)

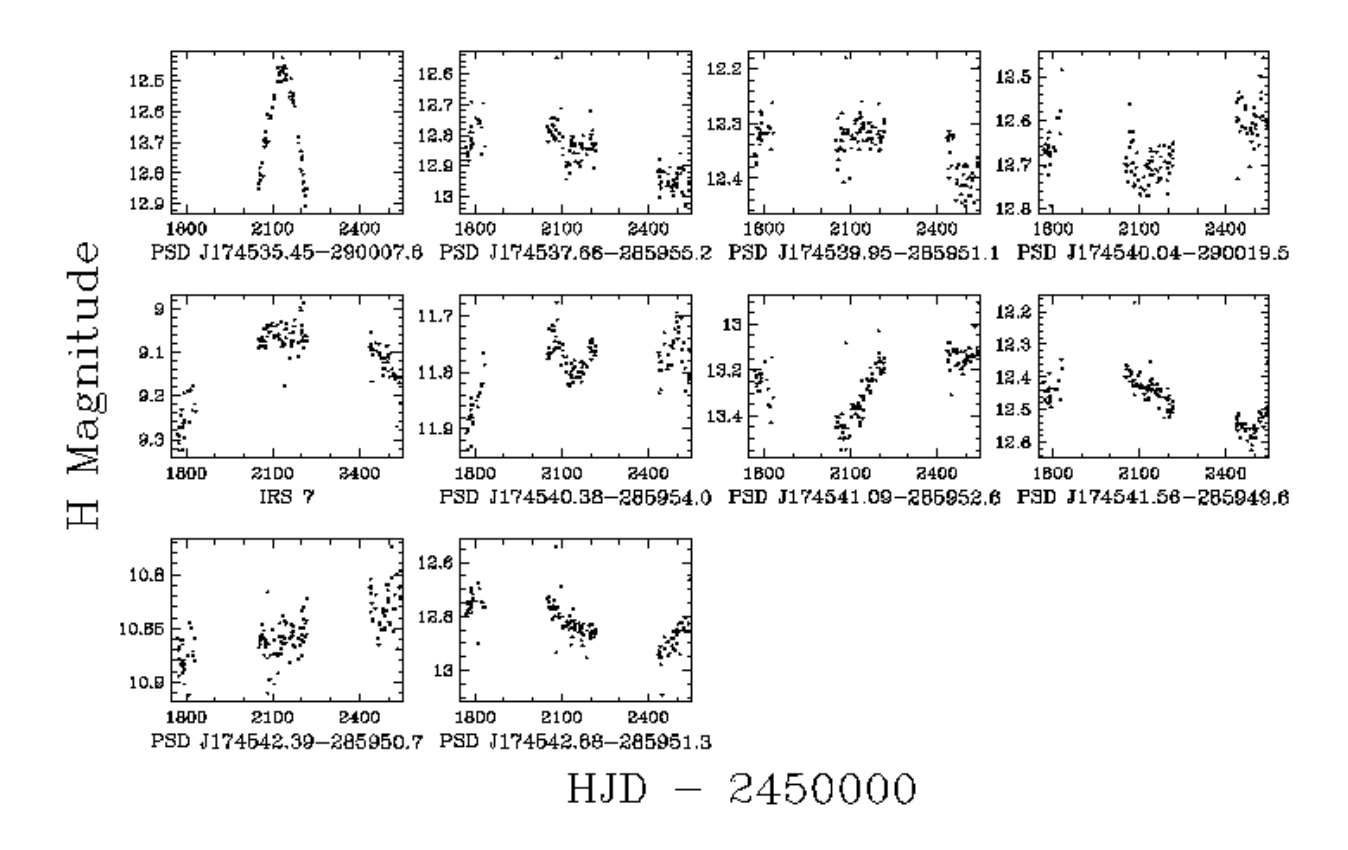


Fig. 6.— Light curves of non-periodic sources detected only in H-band, sorted by RA as in Table 1. Points lying below the magnitude limit (see \S 3) are not included.

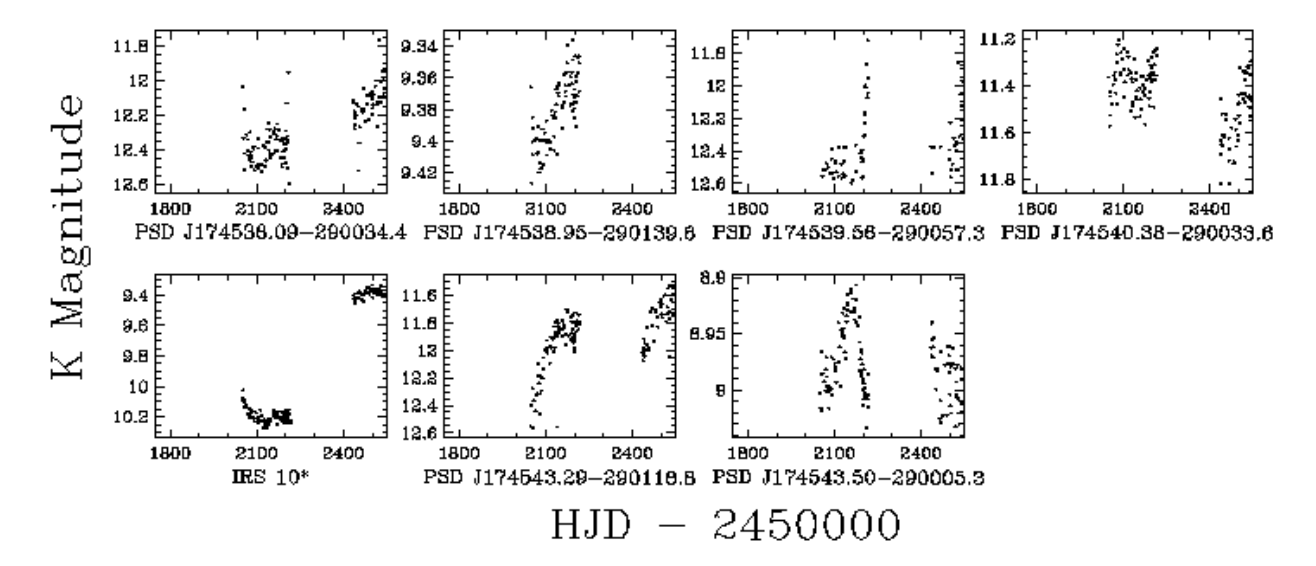


Fig. 7.— Light curves of non-periodic sources detected only in K-band, sorted by RA as in Table 1. Points lying below the magnitude limit (see \S 3) are not included.

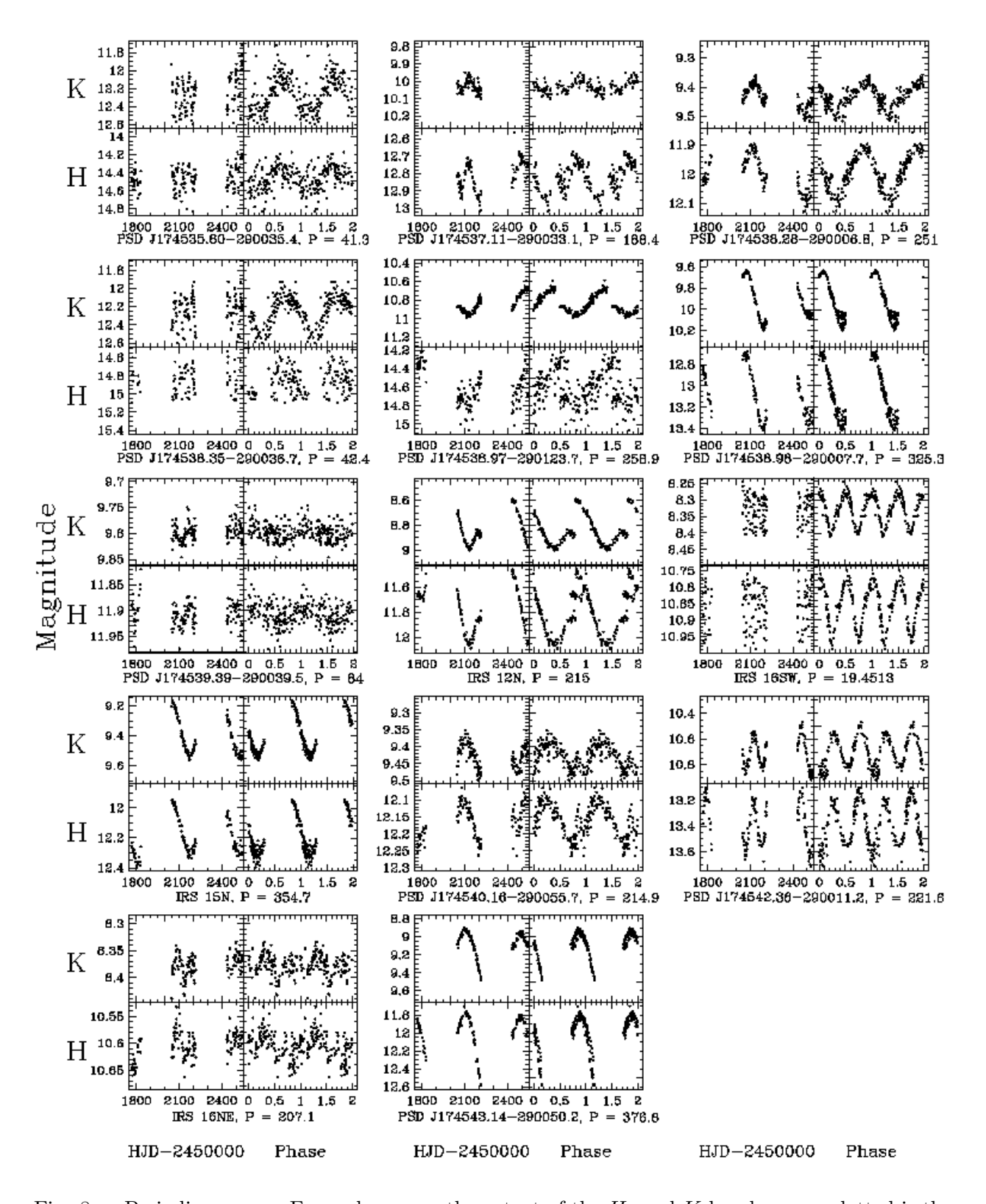


Fig. 8.— Periodic sources. For each source, the extent of the H- and K-band ranges plotted is the same; the unphased light curves are shown in the left panels and the phased light curves are shown in the right panels. Points lying below the magnitude limit (see \S 3) are not included. All given periods P are in days.

Table 1. Catalog of Variable Stars

ID	$\Delta \alpha$ (arcsec)	$\Delta \delta$ (arcsec)	H mag	K mag	Common Names & Notes
PSD J174535.45-290007.6	-68.9	15.1	12.6		
PSD J174535.45-290007.6 PSD J174535.89-290113.5	-68.9 -62.2	-50.8	12.0 14.2	10.9	
PSD J174535.89-290113.5 PSD J174535.98-290011.5	-62.2 -60.9	-30.8 11.3	14.2 12.1	9.7	
PSD J174536.18-290047.6	-57.9	-24.9	12.1 12.4	9.6	
PSD J174536.53-290125.9	-57.9 -52.6	-24.9 -56.8	12.4 11.9	9.5	
PSD J174536.63-290015.4	-52.0 -51.2	-30.8 7.3	10.7	8.8	
PSD J174536.85-290114.5	-31.2 -47.8	-51.8	13.1	10.1	
PSD J174536.97-290138.0	-46.2	-75.3	15.0	10.1	
PSD J174536.97-290019.4	-46.2 -46.1	-73.3 3.3	12.5	10.2	
PSD J174537.10-290103.9	-44.1	-41.2	13.9	10.8	
PSD J174537.10-290105.9	-44.1 -42.0	-41.2 -23.0	12.6	9.9	V4910 Sgr
PSD J174537.42-290042.2	-39.3	-25.0 -19.5	13.8	10.6	, 1010 081
PSD J174537.52-290042.2	-37.9	-13.3 -23.4	14.5	10.6	
PSD J174537.52-290041.7	-37.8	-19.0	12.8	10.0	
PSD J174537.66-285955.2	-35.7	27.4	12.7	10.0	
PSD J174537.74-290009.2	-34.4	13.5	13.1	10.2	
PSD J174537.91-290045.9	-32.0	-23.2	12.7	10.0	
PSD J174537.98-290134.4	-30.9	-71.7	9.5	8.6	CXOGC J174537.9-290134
PSD J174537.98-290004.4	-30.9	18.3	12.0	9.2	0110 000 011 1501.15 250101
PSD J174538.02-290102.6	-30.3	-39.9	12.5	9.3	V4911 Sgr; blended
PSD J174538.05-290058.1	-29.7	-35.4	12.7	10.2	
PSD J174538.10-290033.5	-29.0	-10.9	13.3	10.3	
PSD J174538.19-290005.0	-27.7	17.7	12.5	9.7	
PSD J174538.29-290011.1	-26.2	11.6	13.4	9.9	
PSD J174538.61-290054.3	-21.4	-31.6	13.0	9.5	
PSD J174538.74-290012.7	-19.4	10.0	11.1	9.2	
PSD J174538.79-290004.6	-18.8	18.1	11.8	9.3	
PSD J174538.95-290139.6	-16.3	-77.0		9.4	
PSD J174538.99-290102.2	-15.7	-39.6	14.3	12.4	
PSD J174539.09-290039.3	-14.2	-16.6	12.7	9.8	blended
PSD J174539.23-290036.3	-12.1	-13.6	14.1	10.8	
PSD J174539.31-290016.3	-11.0	6.4	11.6	9.2	CXOGC J174539.3-290016
PSD J174539.31-290054.1	-11.0	-31.5	12.6	10.0	
PSD J174539.36-290055.6	-10.1	-33.0	13.0	10.5	
PSD J174539.39-290014.6	-9.7	8.0	10.9	8.4	blended
PSD J174539.45-290056.6	-8.8	-33.9	12.4	9.1	blended
PSD J174539.56-290057.3	-7.1	-34.7		12.5	
PSD J174539.58-290049.5	-6.9	-26.8	12.4	9.6	
PSD J174539.60-290107.6	-6.6	-44.9	15.3	11.8	H past threshold
PSD J174539.73-290050.2	-4.6	-27.5	12.5	9.9	

Table 1—Continued

ID	$\Delta \alpha$ (arcsec)	$\Delta \delta$ (arcsec)	H mag	K mag	Common Names & Notes
	. , ,		10.5		TDG 00
PSD J174539.75-290055.5	-4.3	-32.8	12.5	9.6	IRS 22
PSD J174539.76-290026.4	-4.1	-3.7	14.1	10.6	IRS 34W
PSD J174539.77-290043.9	-4.0	-21.2	12.1	9.6	
PSD J174539.79-290008.5	-3.6	14.2	11.4	8.5	TDG 10F
PSD J174539.79-290029.9	-3.6	-7.2	13.2	10.6	IRS 13E
PSD J174539.83-290053.9	-3.1	-31.2	9.6	7.6	blended
PSD J174539.86-290024.7	-2.7	-2.0	10.0	10.5	
PSD J174539.86-290019.7	-2.6	3.0	12.8	10.0	
PSD J174539.90-290034.5	-2.1	-11.8	13.3	10.6	blended
PSD J174539.91-290011.0	-2.0	11.7	12.5	9.9	CXOGC J174539.9-290012
PSD J174539.93-290024.9	-1.6	-2.3	13.9	10.5	
PSD J174539.95-285951.1	-1.4	31.6	12.2		
PSD J174539.95-290110.8	-1.3	-48.2	14.2	10.2	
PSD J174539.99-290016.5	-0.7	6.2	12.1	9.8	IRS 15SW
PSD J174540.02-290037.2	-0.3	-14.5	11.8	9.4	IRS 14SW
PSD J174540.04-290018.0	0.0	4.7	12.3	10.3	IRS 15NE
PSD J174540.04-290022.7	0.0	0.0	9.0		IRS 7, saturated in K
PSD J174540.04-290027.0	0.0	-4.3	11.6	9.3	IRS 16NW
PSD J174540.04-290019.5	0.1	3.2	12.6		
PSD J174540.06-290112.1	0.4	-49.4	12.0	9.9	
PSD J174540.11-290036.4	1.0	-13.7	11.8	9.1	IRS 14NE
PSD J174540.21-290043.2	2.6	-20.5	14.1	10.7	
PSD J174540.21-290056.3	2.6	-33.6	15.6		
PSD J174540.31-285953.8	4.1	28.9	13.0		
PSD J174540.31-290039.5	4.1	-16.8	12.3	9.4	
PSD J174540.37-285954.0	5.0	28.7	11.7		blended
PSD J174540.38-290033.6	5.1	-10.9		11.4	
PSD J174540.45-290036.3	6.2	-13.6	13.8	11.1	CXOGC J174540.4-290036
PSD J174540.47-290034.6	6.4	-11.9	11.3	8.6	IRS 9, blended
PSD J174540.58-290026.7	8.2	-4.0	11.9	9.2	IRS 1NE
PSD J174540.64-290023.6	7.8	-1.4		10.2	IRS 10*, blended ^a
PSD J174540.83-290034.0	11.9	-11.4	12.2	9.1	IRS 28
PSD J174540.84-290027.0	12.0	-4.4	12.0	9.5	IRS 32
PSD J174541.04-290022.7	15.0	0.0	11.1	8.5	
PSD J174541.09-285952.6	15.8	30.1	13.2		
PSD J174541.17-290046.9	17.0	-24.2	10.7	7.9	IRS 19, blended
PSD J174541.20-290039.0	17.4	-16.3	11.6	9.1	
PSD J174541.27-290049.9	18.5	-27.2	12.8	9.6	
PSD J174541.35-290033.0	19.6	-10.4	13.2	10.2	
PSD J174541.36-290022.7	19.8	-0.1	11.9	9.4	

REFERENCES

- Alard, C. 2000, A&AS, 144, 363
- Alard, C. & Lupton, R. H. 1998, ApJ, 503, 325
- Blackman, E. G., Frank, A., Markiel, J. A., Thomas, J. H., & Van Horn, H. M. 2001, Nature, 409, 485
- Blum, R. D., Ramírez, S. V., Sellgren, K., & Olsen, K. 2003, ApJ, 597, 323
- Blum, R. D., Sellgren, K., & DePoy, D. L. 1996a, ApJ, 470, 864
- —. 1996b, AJ, 112, 1988
- Clark, J. S., Larionov, V. M., & Arkharov, A. 2005, A&A, 435, 239
- Deguchi, S., Fujii, T., Miyoshi, M., & Nakashima, J.-I. 2002, PASJ, 54, 61
- DePoy, D. L., Atwood, B., Belville, S. R., Brewer, D. F., Byard, P. L., Gould, A., Mason, J. A., O'Brien, T. P., Pappalardo, D. P., Pogge, R. W., Steinbrecher, D. P., & Teiga, E. J. 2003, in Instrument Design and Performance for Optical/Infrared Ground-based Telescopes. Edited by Iye, Masanori; Moorwood, Alan F. M. Proceedings of the SPIE, Volume 4841, pp. 827-838 (2003)., ed. M. Iye & A. F. M. Moorwood, 827-838
- DePoy, D. L., Pepper, J., Pogge, R. W., Stutz, A., Pinsonneault, M., & Sellgren, K. 2004, ApJ, 617, 1127
- Efstathiou, G. 2000, MNRAS, 317, 697
- Eisenhauer, F., Genzel, R., Alexander, T., Abuter, R., Paumard, T., Ott, T., Gilbert, A., Gillessen, S., Horrobin, M., Trippe, S., Bonnet, H., Dumas, C., Hubin, N., Kaufer, A., Kissler-Patig, M., Monnet, G., Ströbele, S., Szeifert, T., Eckart, A., Schödel, R., & Zucker, S. 2005, ApJ, 628, 246
- Genzel, R., Thatte, N., Krabbe, A., Kroker, H., & Tacconi-Garman, L. E. 1996, ApJ, 472, 153
- Glass, I. S., Matsumoto, S., Carter, B. S., & Sekiguchi, K. 2001, MNRAS, 321, 77
- Hartman, J. D., Bakos, G., Stanek, K. Z., & Noyes, R. W. 2004, AJ, 128, 1761
- Hindsley, R. B. & Bell, R. A. 1990, ApJ, 348, 673
- Jackson, J. M., Geis, N., Genzel, R., Harris, A. I., Madden, S., Poglitsch, A., Stacey, G. J., & Townes, C. H. 1993, ApJ, 402, 173
- Karovska, M., Schlegel, E., Hack, W., Raymond, J. C., & Wood, B. E. 2005, ApJ, 623, L137
- Kastner, J. H. & Soker, N. 2004a, ApJ, 608, 978

Table 1—Continued

ID	$\Delta \alpha$ (arcsec)	$\Delta \delta$ (arcsec)	H mag	K mag	Common Names & Notes
PSD J174541.39-290126.6	20.3	-64.0	13.9	9.6	
PSD J174541.56-285949.6	22.9	33.1	12.4		
PSD J174541.59-290023.0	23.3	-0.4	13.7	10.8	
PSD J174541.75-290004.6	25.7	18.1	12.1	9.0	
PSD J174541.75-290013.0	25.7	9.7	12.3	9.3	
PSD J174542.01-290024.4	29.6	-1.8	13.2	10.0	
PSD J174542.13-290045.8	31.5	-23.1	13.5	10.3	
PSD J174542.39-285950.7	35.3	32.0	10.8		
PSD J174542.60-290103.9	38.5	-41.2	14.3	11.0	
PSD J174542.72-285957.4	40.2	25.3	10.5	7.7	V4928 Sgr, blended
PSD J174542.76-290125.5	40.9	-62.8	10.7	8.7	
PSD J174542.88-285951.3	42.6	31.4	12.7		
PSD J174542.92-285958.4	43.3	24.3	14.2	11.8	
PSD J174543.01-290011.9	44.6	10.7	10.8	8.5	
PSD J174543.19-290013.0	47.2	9.7	10.9	8.2	V4930 Sgr, blended
PSD J174543.29-290118.8	48.8	-56.2		11.9	
PSD J174543.31-290014.3	49.1	8.4	14.8	12.6	
PSD J174543.50-290005.3	52.0	17.4		9.0	

Note. — Non-perioidic variable sources, sorted by RA. $\Delta\alpha$ and $\Delta\delta$ are with respect to IRS 7 at $(\alpha, \delta) = 17^{\rm h}45^{\rm m}40.04^{\rm s}, -29^{\circ}00'22.7''$ J2000.0 (Blum et al. 2003). In these coordinates, Sgr A* $((\alpha, \delta) = 17^{\rm h}45^{\rm m}40.04^{\rm s}, -29^{\circ}00'28.1''$ J2000.0) is at $(\Delta\alpha, \Delta\delta) = (0.0'', -5.4'')$. The magnitudes listed are the fiducial magnitudes calculated from the ISIS reference image (see § 3); these magnitudes are *not* mean magnitudes.

^aThis position is from Ott et al. (1999).

Table 2. Catalog of Periodic Variable Stars

ID	$\Delta \alpha$ (arcsec)	$\Delta \delta$ (arcsec)	H mag	K mag	Period (days)	Notes
PSD J174535.60-290035.4	-66.6	-12.7	14.5	12.3	41.3 ± 0.5	CXOGC J174535.6-290034
PSD J174537.11-290033.1	-44.0	-10.4	10.0	12.8	188.4 ± 6.8	
PSD J174538.28-290006.8	-26.5	15.9	11.9	9.3	251.0 ± 8.4	
PSD J174538.35-290036.7	-25.5	-14.0	14.9	12.1	42.4 ± 0.8	
PSD J174538.97-290123.7	-16.1	-60.9	14.6	10.8	258.9 ± 8.3	
PSD J174538.98-290007.7	-16.0	15.0	13.0	9.9	325.3 ± 3.5	
PSD J174539.39-290039.5	-9.8	16.8	11.9	9.8	84.0 ± 1.3	
PSD J174539.79-290035.2	-3.8	-12.5	11.8	8.8	215.0 ± 2.4	IRS 12N, very blended
PSD J174540.12-290029.6	1.2	-6.8	10.8	8.3	19.4513 ± 0.0011	IRS 16SW
PSD J174540.13-290016.8	1.3	5.9	12.1	9.4	354.7 ± 4.2	IRS 15N, blended
PSD J174540.16-290055.7	1.7	-32.9	12.1	9.3	214.9 ± 2.6	CXOGC J174540.1-290055
PSD J174542.36-290011.2	34.8	11.6	13.4	10.6	221.6 ± 2.6	
PSD J174540.25-290027.2	3.2	-4.6	10.5	8.3	207.1 ± 6.1	IRS 16NE
PSD J174543.14-290050.2	46.5	-27.5	12.0	9.1	376.8 ± 4.1	blended

Note. — $\Delta \alpha$ and $\Delta \delta$ are with respect to IRS 7 at $(\alpha, \delta) = 17^{\rm h}45^{\rm m}40.04^{\rm s}$, $-29^{\circ}00'22.7''$ J2000.0. The magnitudes listed are the fiducial magnitudes calculated from the ISIS reference image (see § 3); these magnitudes are *not* mean magnitudes. Except for IRS 16SW, the listed uncertainties on the periods roughly correspond to FWHM of the AoV peak (see § 3. For IRS 16SW, the listed period and uncertainty are from Peeples et al. (2007); see also §§ 5.10.

Table 3. Near-infrared Photometric Surveys of the Galactic Center

Survey	Field of View	Time Sampling	Wavelength	Notes & Variable Sources
Tamura et al. (1996)	$24'' \times 24''$	1991, 1992, 1993; 3 epochs	K	IRS 9, 10*, 12N, 14SW, 28
Blum et al. (1996a)	central $\sim 2'$	May 1993–April 1995; 5–8 epochs	J,H,K,L	IRS 7, 9, 12N
Ott et al. (1999)	$20^{\prime\prime} \times 20^{\prime\prime}$	August 1992–May 1998; ~ 40 epochs	K	IRS 7, 9, 10*, 12N, 16SW and potentially IRS 1NE, 6, 14SW
Glass et al. (2001)	$24' \times 24'$	1994–1997; ~ 30 epochs	K	only large-amplitude, periodic variability
Rafelski et al. (2007)	$5'' \times 5''$	1995–2005; 50 epochs	K	IRS 16SW, 16NW, 16CC, 19N, and 12 S stars

Note. — For reference, 1'' at 7.6 kpc (Eisenhauer et al. 2005, Galactocentric distance) corresponds to 0.0368 pc projected; 1' corresponds to 2.211 pc projected.

Table 4. Summary of Sources Discussed in \S 5

ID	Figure	Period	Classification	Alternate Name
IRS 1NE	5(d)			PSD J174540.58-290026.7
IRS 7	6		LPV	PSD J174540.04-290022.7
IRS 9	5(d)		LPV	PSD J174540.47-290034.6
IRS 10*	7		OH/IR, X-ray source	PSD J174540.64-290023.6
IRS 12N	8	215.0 ± 2.4	LPV	PSD J174539.79-290035.2
IRS 14SW	5(d)			PSD J174540.02-290037.2
IRS 14NE	5(d)		AGB	PSD J174540.11-290036.4
IRS 15SW	5(c)		WR	PSD J174539.99-290016.5
IRS 16NE	8	207.1 ± 6.1	LBV?	PSD J174540.25-290027.2
IRS 16SW	8	19.451 ± 0.001	binary	PSD J174540.12-290029.6
IRS 28	5(d)			PSD J174540.83-290034.0
IRS 34W	5(c)		LBV?	PSD J174539.76-290026.4
V4910 Sgr	5(a)			PSD J174537.24-290045.7
V4911 Sgr	5(b)		SiO maser?	PSD J174538.02-290102.6
V4928 Sgr	5(e)		OH/IR	PSD J174542.72-285957.4
V4930 Sgr	5(e)		Mira	PSD J174543.19-290013.0
PSD J174535.60-290035.4	8	41.3 ± 0.5		
PSD J174538.34-290036.7	8	42.4 ± 0.8	binary??	
PSD J174538.98-290007.7	8	325.3 ± 3.5	LPV?	
PSD J174537.98-290134.4	5(a)		X-ray source	
PSD J174539.31-290016.3	5(b)		X-ray source	
PSD J174540.16-290055.7	8	221.6 ± 2.6	variable X-ray	
PSD J174541.39-290126.6	5(e)		OH/IR	
PSD J174542.36-290011.2	8	221.6 ± 2.6		
PSD J174543.14-290050.2	8	376.8 ± 4.1		

Note. — Sources are sorted in the order they are discussed in \S 5; all given periods are in days.

- —. 2004b, ApJ, 616, 1188
- Krabbe, A., Genzel, R., Eckart, A., Najarro, F., Lutz, D., Cameron, M., Kroker, H., Tacconi-Garman, L. E., Thatte, N., Weitzel, L., Drapatz, S., Geballe, T., Sternberg, A., & Kudritzki, R. 1995, ApJ, 447, L95+
- Lacy, J. H., Townes, C. H., & Hollenbach, D. J. 1982, ApJ, 262, 120
- Laney, C. D. & Stobie, R. S. 1994, MNRAS, 266, 441
- Levine, D. A., Figer, D. F., Morris, M., & McLean, I. S. 1995, ApJ, 447, L101+
- Lindqvist, M., Winnberg, A., & Forster, J. R. 1990, A&A, 229, 165
- Lindqvist, M., Winnberg, A., Habing, H. J., & Matthews, H. E. 1992, A&AS, 92, 43
- Martins, F., Trippe, S., Paumard, T., Ott, T., Genzel, R., Rauw, G., Eisenhauer, F., Gillessen, S., Maness, H., & Abuter, R. 2006, ApJ, 649, L103
- Menten, K. M., Reid, M. J., Eckart, A., & Genzel, R. 1997, ApJ, 475, L111+
- Muno, M. P., Arabadjis, J. S., Baganoff, F. K., Bautz, M. W., Brandt, W. N., Broos, P. S., Feigelson, E. D., Garmire, G. P., Morris, M. R., & Ricker, G. R. 2004, ApJ, 613, 1179
- Najarro, F., Krabbe, A., Genzel, R., Lutz, D., Kudritzki, R. P., & Hillier, D. J. 1997, A&A, 325, 700
- Nayakshin, S. & Sunyaev, R. 2005, MNRAS, 364, L23
- Ott, T., Eckart, A., & Genzel, R. 1999, ApJ, 523, 248
- Paumard, T., Genzel, R., Martins, F., Nayakshin, S., Beloborodov, A. M., Levin, Y., Trippe, S., Eisenhauer, F., Ott, T., Gillessen, S., Abuter, R., Cuadra, J., Alexander, T., & Sternberg, A. 2006, ApJ, 643, 1011
- Peeples, M. S., Bonanos, A. Z., DePoy, D. L., Stanek, K. Z., Pepper, J., Pogge, R. W., Pinsonneault, M. H., & Sellgren, K. 2007, ApJ, 652, L61
- Rafelski, M., Ghez, A. M., Hornstein, S. D., Lu, J. R., & Morris, M. 2007, ArXiv Astrophysics e-prints
- Reid, M. J. & Moran, J. M. 1981, ARA&A, 19, 231
- Samus, N. N. & Durlevich, O. V. 2004, VizieR Online Data Catalog, 2250, 0
- Scannapieco, E., Silk, J., & Bouwens, R. 2005, ApJ, 635, L13
- Scargle, J. D. 1982, ApJ, 263, 835

Schlegel, D. J., Finkbeiner, D. P., & Davis, M. 1998, ApJ, 500, 525

Schwarzenberg-Czerny, A. 1996, ApJ, 460, L107+

Scoville, N. Z., Stolovy, S. R., Rieke, M., Christopher, M., & Yusef-Zadeh, F. 2003, ApJ, 594, 294

Silk, J. 1997, ApJ, 481, 703

Sjouwerman, L. O. 1997, PhD thesis, AA(Onsala Space Observatory, Sweden

Sjouwerman, L. O., Lindqvist, M., van Langevelde, H. J., & Diamond, P. J. 2002, A&A, 391, 967

Skrutskie, M. F., Cutri, R. M., Stiening, R., Weinberg, M. D., Schneider, S., Carpenter, J. M., Beichman, C., Capps, R., Chester, T., Elias, J., Huchra, J., Liebert, J., Lonsdale, C., Monet, D. G., Price, S., Seitzer, P., Jarrett, T., Kirkpatrick, J. D., Gizis, J. E., Howard, E., Evans, T., Fowler, J., Fullmer, L., Hurt, R., Light, R., Kopan, E. L., Marsh, K. A., McCallon, H. L., Tam, R., Van Dyk, S., & Wheelock, S. 2006, AJ, 131, 1163

Soker, N. & Zoabi, E. 2002, MNRAS, 329, 204

Sterken, C. & Jaschek, C. 1996, Light Curves of Variable Stars, A Pictorial Atlas (Light Curves of Variable Stars, A Pictorial Atlas, ISBN 0521390168, Cambridge University Press, 1996.)

Stetson, P. B. 1987, PASP, 99, 191

—. 1992, JRASC, 86, 71

Tamura, M., Werner, M. W., Becklin, E. E., & Phinney, E. S. 1996, ApJ, 467, 645

Trippe, S., Martins, F., Ott, T., Paumard, T., Abuter, R., Eisenhauer, F., Gillessen, S., Genzel, R., Eckart, A., & Schödel, R. 2006, A&A, 448, 305

van der Hucht, K. A. 2001, New Astronomy Review, 45, 135

Wood, P. R., Habing, H. J., & McGregor, P. J. 1998, A&A, 336, 925

This preprint was prepared with the AAS LATEX macros v5.2.